Journal of Biosciences and Medicines, 2026, 14(4), 90-104
https://www.scirp.org/journal/jbm
ISSN Online: 2327-509X
ISSN Print: 2327-5081

Distinct Microbial Niches in Urinary Stones and Paired Urine Samples Characterized by 16S rRNA Sequencing

Shuyang Yu[1,2], Tingting Liang[2], Yuan Gao[2], Heng Li[2], Zhemin Zhou[3], Xuejie Wu[1*]

[1]Suzhou BenQ Medical Center, Suzhou, China
[2]Suzhou Key Laboratory of Geriatric Intelligent Nursing and Health Preservation, School of Nursing, Suzhou Medical College of Soochow University, Suzhou, China
[3]MOE Key Laboratory of Geriatric Diseases and Immunology, Cancer Institute, Suzhou Medical College, Soochow University, Suzhou, China
Email: *drwxj@sina.com

How to cite this paper: Yu, S.Y., Liang, T.T., Gao, Y., Li, H., Zhou, Z.M. and Wu, X.J. (2026) Distinct Microbial Niches in Urinary Stones and Paired Urine Samples Characterized by 16S rRNA Sequencing. *Journal of Biosciences and Medicines*, **14**, 90-104.
https://doi.org/10.4236/jbm.2026.144008

Received: February 26, 2026
Accepted: April 10, 2026
Published: April 13, 2026

Abstract

Distinct yet linked microbial ecosystems in urinary stones and urine may influence stone pathogenesis. This study characterized the microbiome of 59 paired stone and urine samples using 16S rRNA sequencing and clinical correlation analysis. Results showed that stone biofilms were enriched with environmental bacteria (e.g., Christensenella, Chromobacterium), whereas urine primarily harbored uropathogens (e.g., Klebsiella, Acinetobacter). Significant gender and pathogen-specific patterns emerged, with Mycoplasma/Ureaplasma infections showing female predominance (85.7%) and Group 2 showing the highest median crystalluria value (57.8 counts) together with the lowest median urinary pH (6.19), although these observations were interpreted descriptively and not as statistically significant pairwise associations. Distance metrics (0 - 0.88) demonstrated varying microbial similarity between samples, with closer clustering among stone-associated communities. These findings support ecological differentiation between urinary stones and paired urine, while indicating that mechanistic and causal interpretation requires further validation.

Keywords

Urinary Microbiome, Urolithiasis, 16S rRNA Sequencing, Biofilm, Microbial Ecology, Diagnostic Biomarkers

1. Introduction

Urinary tract infections (UTIs) and urinary stones are prevalent urological con-

ditions that often occur together, with infections promoting stone formation and stones predisposing to infections [1]. According to the World Health Organization (WHO), UTIs affected an estimated 150 million people annually worldwide, with women being disproportionately impacted due to anatomical factors [2].

The microbiota in urine and stones plays a critical role in disease development, yet the interplay between these microbial communities remains poorly characterized. Previous 16S rRNA sequencing studies have revealed diverse urinary bacteria, including *Escherichia coli*, *Proteus mirabilis*, and *Klebsiella pneumoniae* as common pathogens in UTIs [3]. In contrast, urinary stones harbor distinct microbial profiles, often dominated by urease-producing bacteria like *P. mirabilis* in struvite stones [4].

Notably, bacterial colonization patterns vary by niche. *Escherichia coli*, the predominant uropathogen, is frequently detected in UTI-associated urine but rarely in stones, suggesting differences in adhesion and persistence mechanisms [5]. Conversely, *Staphylococcus aureus*, known for biofilm formation, has been found in both urine and calcium oxalate stones, indicating a possible role in stone-related infections [6]. Urease-producing bacteria such as *P. mirabilis* and Klebsiella spp. are particularly enriched in infection stones (e.g., struvite and carbonate apatite), where their enzymatic activity drives stone formation [7]. These findings imply that while some bacteria transiently colonize urine, others possess adaptive traits enabling stone integration. However, the precise transition mechanisms remain unclear.

Advances in high-throughput sequencing have deepened our understanding of urological microbiomes, yet key questions persist. Some studies suggest stone microbiota mirror urinary bacteria, while others report significant divergence between the two environments [8]-[10]. This inconsistency underscores the need for integrated analyses of paired urine-stone samples to clarify microbial transmission and colonization dynamics. Despite progress, the mechanisms underlying microbial shifts between urine and stones remain elusive. This study aims to unravel these dynamics through comprehensive paired-sample analysis.

2. Materials and Methods

2.1. Clinical Background

The study included 59 paired urinary stone and urine samples collected from patients diagnosed with urolithiasis at Suzhou BenQ Medical Center between November 2023 and April 2024. All patients provided informed consent, and the study was approved by the Ethics Committee of Soochow University (Reference 2020CS017). All samples were collected and processed using sterile handling procedures. For downstream comparison, pathogen-dominated groups were defined according to the dominant pathogen profile: Group 1, Mycoplasma/Ureaplasma; Group 2, Pseudomonas; Group 3, *E. coli*; and Group 4, *Staphylococcus aureus*.

2.2. Specimen Collection

Fresh urine samples and stone fragments were collected during surgical proce-

dures. Stones were aseptically scraped to obtain biofilm samples, while urine samples were centrifuged to pellet microbial cells [11]. All specimens were stored at −80˚C until DNA extraction.

2.3. DNA Extraction

The urine samples and stone-scraped swabs were processed for microbial analysis. Urine was centrifuged to pellet microbial cells, while swab tips were vortexed in PBS to dislodge adherent bacteria. Genomic DNA was extracted using the MagaBio Soil/Feces Genomic DNA Purification Kit (Bioer Technology, Hangzhou, China), with modifications for low-biomass samples [12] [13]. DNA purity and concentration were assessed spectrophotometrically (NanoDrop ND-1000, Thermo Fisher Scientific) based on A260/A280 ratios. All extracts were normalized to 1 ng/μl (to account for lower microbial biomass) and stored at −20˚C.

2.4. Bacterial 16S rRNA Sequencing

The hypervariable V3-V4 regions of bacterial 16S rRNA genes were amplified using barcoded primers (Invitrogen). PCR reactions (50 μl total volume) contained: 25 μl Taq polymerase mix (Takara Bio), 1 μl each of forward and reverse primers (10 mM), and 3 μl template DNA. Thermal cycling conditions were: initial denaturation at 94˚C for 30 sec; 30 cycles of 94˚C (30 sec), 52˚C (30 sec), and 72˚C (30 sec); with a final extension at 72˚C for 10 min. PCR products were verified by 1% agarose gel electrophoresis, pooled in equimolar ratios (GeneTools Analysis Software, SynGene), and sequenced on an Illumina MiSeq (PE300, MAGIGENE Genomic Institute).

2.5. Bioinformatic Analyses of Genomic Data

The raw paired-end sequencing data were processed using BBmerge (BBtools suite v38.94) with the following parameters: "loose = t mininsert = 120 mininsert0 = 100 qtrim2 = t qout = 33 entropy = t maxns = 0 trimq = 10" to merge overlapping reads while maintaining high accuracy. Quality filtering was performed using Vsearch v2.18.0 with a maximum expected error rate of 0.02 (fastq_maxee_rate = 0.02) to remove low-quality sequences [14]. For consistency of downstream analysis, the primary feature unit reported in this study was amplicon sequence variants (ASVs). High-quality reads were denoised with the "cluster_unoise" module, and potential sequencing artifacts were further removed by chimera detection using "uchime3_denovo" to generate the refined ASV table.

For taxonomic classification, ASVs were aligned against the SILVA 138.1 16S rRNA database using BLASTn, retaining only matches with ≥85% sequence identity over ≥50% of the read length. Final taxonomic assignments were determined using a hybrid lowest common ancestor (LCA) approach to ensure robust classification accuracy. Microbial community diversity was assessed using QIIME 1.9.1, which calculated multiple alpha diversity indices including observed richness, Chao1, Shannon, Simpson, ACE, Goods-coverage, and PD_whole_tree [15]. These

metrics were visualized through rarefaction curves, rank-abundance plots, and species accumulation curves generated in R v4.1.2.

Statistical comparisons of alpha diversity between sample groups were performed using both parametric (t-test) and non-parametric (Wilcoxon) tests as appropriate based on data distribution characteristics. Beta diversity analysis incorporated principal coordinate analysis (PCoA), principal component analysis (PCA), and non-metric multidimensional scaling (NMDS) using R's stats, ggplot2, and vegan packages. Differences in beta diversity metrics were evaluated using both parametric and non-parametric statistical approaches. Differential abundance analysis was conducted using STAMP software with default score filtering parameters, supplemented by group-wise t-tests in R for identifying significantly different taxa [16]. All visualizations were generated using R's advanced plotting capabilities to ensure clear representation of the complex microbial community data.

3. Results

3.1. Demographic Characteristics and Clinical Parameters

The comparative analysis of clinical and urinary parameters across the four pathogen-defined groups revealed distinct microbial-associated profiles. Demographic analysis showed significant gender disparities, with Group 1 (*Mycoplasma*/*Ureaplasma*-dominated infections) exhibiting a striking female predominance (85.7%) compared to Group 2 (*Pseudomonas*-dominated, 81.5% male; $p < 0.001$). This gender distribution pattern was similarly significant between Group 1 and Group 4 (*Staphylococcus aureus*-dominated, $p = 0.015$), suggesting potential pathogen-specific tropisms for different host sexes.

Urinary inflammatory markers demonstrated clear group-specific patterns. Group 1 showed markedly elevated leukocyte counts (median 535.6, IQR 911.7) compared to all other groups (all $p \leq 0.012$), indicating a particularly robust inflammatory response to Mycoplasma/Ureaplasma infections. Biochemical analysis revealed that Group 2 maintained significantly lower urinary pH (median 6.19) than Group 1 (median 6.79, $p = 0.037$), whereas the crystal-examination result was retained as a descriptive pattern rather than a statistically significant pairwise difference. Group 2 showed the highest median crystal count (57.8, IQR 1.1) and Group 4 showed the lowest median value (0.2, IQR 0.2), but this contrast should be interpreted cautiously in light of the non-significant pairwise results shown in Table 1. The group-level clinical and laboratory characteristics are summarized in Table 2.

Microbiological and cellular findings provided further differentiation between groups. While bacterial and fungal loads showed no significant differences, epithelial cell patterns varied meaningfully. Group 4 displayed the highest squamous epithelial cell counts (median 9.3, IQR 1.2), whereas Group 3 (*E. coli*-dominated) showed elevated small round epithelial cells (median 17.4, IQR 11), potentially indicating different sites or mechanisms of epithelial damage. Group 1 demon-

strated numerically higher red blood cell counts (median 17,996, IQR 8069), though this did not reach statistical significance compared to other groups.

Table 1. Statistical comparison of clinical and urinary parameters across pathogen-defined groups. The table presents p-values from pairwise comparisons (Wilcoxon/t-tests) of demographic and urinary parameters among four pathogen-dominated groups: Group 1: Mycoplasma/Ureaplasma-dominant infections (female-predominant, high inflammation). Group 2: Pseudomonas-dominant infections (male-predominant, lower urinary pH and higher median crystal-examination value in descriptive analysis). Group 3: *E. coli*-dominant infections. Group 4: *Staphylococcus aureus*-dominant infections. Significant differences (*p* < 0.05, marked with ※) highlight group-specific patterns, such as gender disparity (Group 1 vs. 2, *p* < 0.001), urinary pH (Group 1 vs. 2, *p* = 0.037), and leukocyte counts (Group 1 vs. others, *p* ≤ 0.012).

Indicators	1v2	1v3	1v4	2v3	2v4	3v4
Gender	< 0.001※	0.147	0.015※	0.116	0.332	0.448
Length of stay	0.06	0.583	0.075	0.264	0.893	0.271
Conductivity	0.829	0.333	0.607	0.332	0.659	0.555
Urine osmolality	0.837	0.34	0.614	0.326	0.66	0.558
pH	0.037※	0.584	0.122	0.188	0.644	0.382
Urine specific gravity	0.654	0.633	0.643	0.315	0.93	0.333
White blood cell count	0.001※	0.012※	0.001※	0.959	0.586	0.74
Red blood cell count	0.223	0.324	0.118	0.946	0.504	0.687
Bacterial count	0.827	0.795	0.807	0.6	0.945	0.602
Yeast count	0.989	0.963	0.37	0.965	0.227	0.422
Epithelial cell count	0.342	0.498	0.714	0.952	0.507	0.684
Squamous cells	0.575	0.86	0.433	0.756	0.696	0.582
Small round cells	0.512	0.488	0.573	0.811	0.119	0.194
Cases count	0.157	0.119	0.055	0.548	0.352	0.916
Crystal examination	0.588	0.748	0.659	0.367	0.208	0.95
Mucus strands	0.664	0.062	0.133	0.058	0.125	0.503
Creatinine (semiquantitative)	0.503	0.135	0.342	0.221	0.626	0.44

Table 2. Clinical and laboratory characteristics of pathogen-defined groups. Detailed median values (IQR) for each group: Group 1 (n = 10): Elevated leukocytes (median 535.6, IQR 911.7), female predominance (85.7%). Group 2 (n = 27): Low urinary pH (median 6.19), higher median crystal-examination value (median 57.8 counts), male predominance (81.5%). Group 3 (n = 10): Intermediate profiles with elevated small round epithelial cells (median 17.4). Group 4 (n = 12): lower median crystal-examination value (median 0.2 counts). Consistent parameters (e.g., conductivity, osmolality) suggest microbial identity drives phenotypic variation.

Indicators	1 (n = 10)	2 (n = 27)	3 (n = 10)	4 (n = 12)
Male, n (%)	2 (20.0)	22 (81.5)	5 (50)	8 (66.7)
Female, n (%)	8 (80.0)	5 (18.5)	5 (50)	4 (33.3)
Length of stay	47.29 (IQR 34)	28.81 (IQR 19)	40.33 (IQR 79)	27.75 (IQR 13)
Conductivity	16.243 (IQR 12.8)	15.659 (IQR 9.9)	12.8 (IQR 11.3)	14.683 (IQR 10.2)
Urine osmolality	557.14 (IQR 440)	538.07 (IQR 338)	440.67 (IQR 389)	504.75 (IQR 349)
pH	6.786 (IQR 1)	6.185 (IQR 2)	6.583 (IQR 0.8)	6.292 (IQR 1.3)
Urine specific gravity	1.015 (IQR 0.014)	1.017 (IQR 0.011)	1.013 (IQR 0.008)	1.017 (IQR 0.011)

Continued

White blood cell count	535.557 (IQR 911.7)	172.87 (IQR 235.2)	167 (IQR 249.2)	124.767 (IQR 50.9)
Red blood cell count	17996.429 (IQR 8069)	8857.319 (IQR 12034.6)	8319.7 (IQR 21179.1)	4786.058 (IQR 7875.7)
Bacterial count	426.486 (IQR 283.6)	509.015 (IQR 297.1)	297.667 (IQR 293.4)	530.15 (IQR 310.8)
Yeast count	0.443 (IQR 0.5)	0.441 (IQR 0.6)	0.433 (IQR 0.9)	0.283 (IQR 0.5)
Epithelial cell count	13.6 (IQR 27.6)	22.941 (IQR 36.2)	22.317 (IQR 12.3)	17.617 (IQR 17.1)
Squamous cells	1.543 (IQR 0.5)	6.493 (IQR 1.6)	3.583 (IQR 5.1)	9.308 (IQR 1.2)
Small round cells	11.814 (IQR 27.3)	15.83 (IQR 20.2)	17.383 (IQR 11)	7.95 (IQR 9.2)
Cases count	0.8829 (IQR 1.42)	0.5678 (IQR 0.46)	0.4267 (IQR 0.51)	0.3992 (IQR 0.49)
Crystal examination	27.686 (IQR 8.9)	57.848 (IQR 1.1)	4.3 (IQR 12.3)	0.167 (IQR 0.2)
Mucus strands	0.48 (IQR 0.98)	0.4085 (IQR 0.71)	0.07 (IQR 0.14)	0.2 (IQR 0.36)
Creatinine (semiquantitative)	114.29 (IQR 150)	95.93 (IQR 50)	60 (IQR 60)	85 (IQR 125)

Notably, several parameters showed remarkable consistency across groups. Electrolyte markers (conductivity, osmolality), specific gravity, and cast counts maintained stable values regardless of the dominant pathogen, suggesting these factors may be less influenced by specific microbial presence. These findings collectively demonstrate that different uropathogens associate with distinct clinical and laboratory profiles. Mycoplasma/Ureaplasma infections present with pronounced inflammation and female predominance, whereas Group 2 is better described as showing lower urinary pH and a higher median crystal value without firm statistical support for crystalluria differences, while *E. coli* and *S. aureus* show more intermediate patterns with specific epithelial cell signatures.

3.2. Microbial Community Composition and Distribution

The heatmap analysis revealed distinct microbial community structures across the samples (labeled as JS and NY series). *Pseudomonas* and *Staphylococcus* were the most dominant genera, showing high relative abundance in multiple samples (e.g., JS33, NY10, NY23). Other notable genera included *Enterobacteriaceae*, *Proteus*, and *Mycoplasma*, which exhibited variable distribution patterns. Samples such as JS20 and NY18 displayed a higher abundance of *Ureaplasma*, while *Clostridia* and *Dialister* were more prevalent in NY4 and JS11, respectively. The "Others" category, representing low-abundance taxa, was consistently present across all samples, indicating a diverse but unevenly distributed microbial ecosystem. **Figure 1** shows the distribution of the dominant genera across the paired stone and urine samples.

The distance metric (ranging from 0 to 0.88) highlighted varying degrees of microbial similarity between samples. For instance, the samples JS33 and NY10 (distance: 0.22) shared similar microbial profiles, dominated by *Pseudomonas* and *Staphylococcus*. In contrast, JS18 and NY19 (distance: 0.86) showed markedly divergent communities, with the former enriched in *Mycoplasma* and the latter in

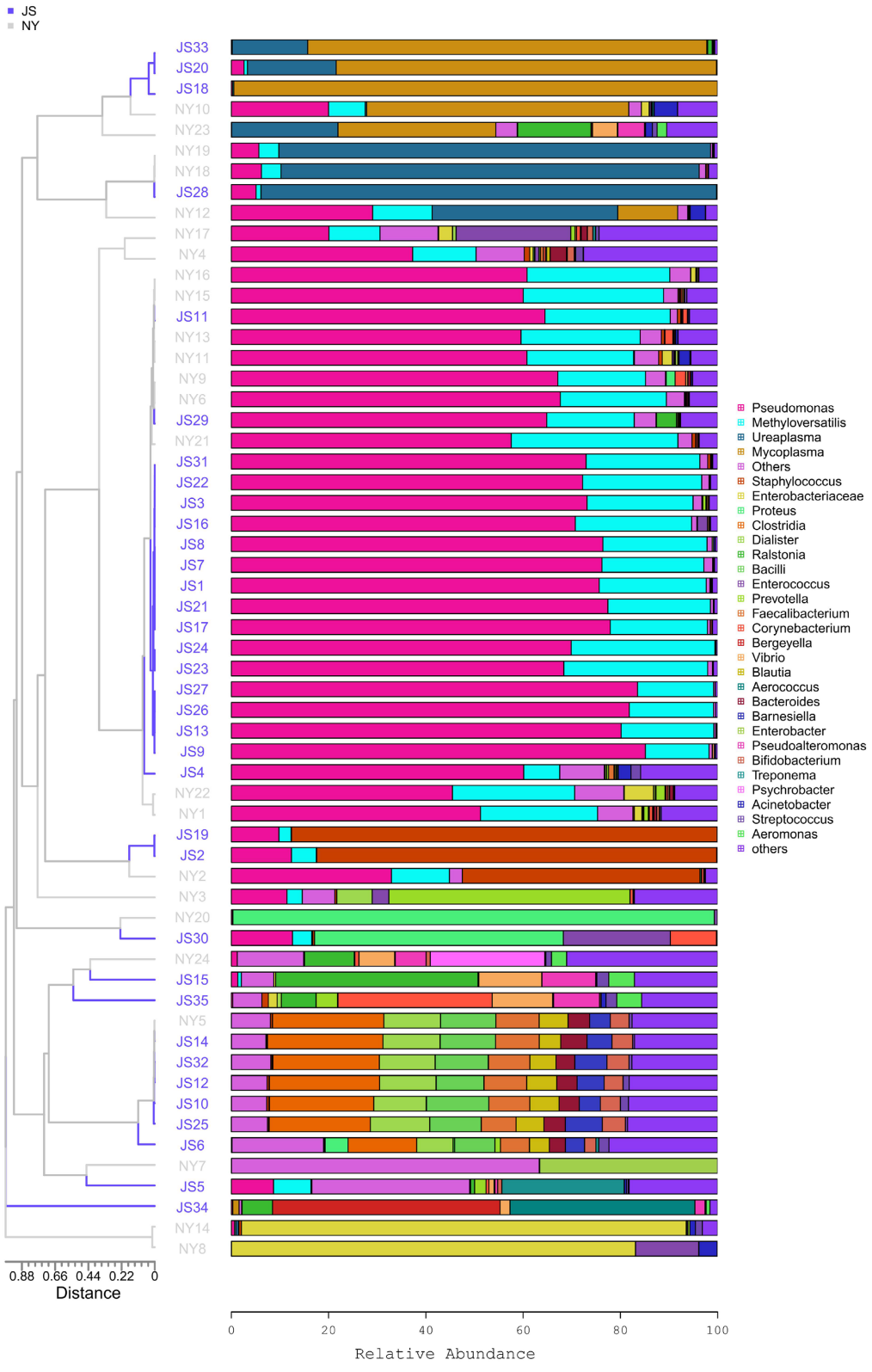

Figure 1. Microbial community composition in urinary stones and paired urine samples. Boxplots showing the relative abundance of dominant bacterial genera in stone (JS series) and urine (NY series) samples. Stone samples (JS) are enriched in environmental taxa (e.g., Christensenella), whereas urine samples (NY) dominate in uropathogens (e.g., Klebsiella).

Enterobacteriaceae. The clustering pattern suggested that samples from the same series (JS or NY) did not always group together, implying that microbial composition was influenced by factors beyond simple sample origin. Gram-negative bacteria (*Pseudomonas*, *Proteus*, *Enterobacteriaceae*) were widespread, particularly in samples with higher distance values (e.g., NY21, JS28), indicating potential polymicrobial infections. Gram-positive bacteria (*Staphylococcus*, *Enterococcus*, *Streptococcus*) were prominent in samples like NY17 and JS7, often co-occurring with other taxa. Anaerobic genera (*Prevotella*, *Dialister*, *Clostridia*) were more abundant in samples with intermediate distances (e.g., NY15, JS9), suggesting niche-specific colonization.

3.3. Diversity Analysis Reveals Distinct But Overlapping Microbiomes between Urine and Stone

Permutational multivariate analysis (PERMANOVA) of the combined dataset indicated that bacterial communities were significantly stratified by sample type (urine vs. stone surface; $p = 0.00067$, $R^2 = 0.16$) and by patient group (JS vs. ENY; $p = 0.00001$, $R^2 = 0.50$), whereas no significant difference was driven by group identity alone ($p = 0.29$). The constrained PCoA (PCoA1 = 32.85 % of total variance) displayed a clear separation of stone-surface swabs toward the negative end of axis 1 and urine samples toward the positive end, with a modest overlap zone at the origin. Notably, JS samples exhibited a tighter cluster along the negative–neutral range, whereas NY samples were more dispersed across the ordination space, suggesting that inter-individual heterogeneity is more pronounced in urine than on stone surfaces. Collectively, these data support niche differentiation between urine and stone-surface communities, but the magnitude of this effect should be interpreted cautiously because a full patient-blocked reanalysis was not available in the current revision. As shown in **Figure 2**, alpha-diversity patterns and constrained ordination support partial but significant separation between the two niches.

3.4. Differentially Abundant Taxa Distinguish JS and NY Cohorts across Urine and Stone Surfaces

At the genus level, 27 bacterial taxa exhibited significant shifts in mean relative abundance (95% CI) between stone matrices (JS) and matched urine (NY). *Klebsiella* was markedly enriched in urine (NY; $\Delta = 3.96\%$, $p = 0.036$), whereas *Christensenella* was almost exclusive to stones (JS; $\Delta = 4.72\%$, $p = 0.047$). Conversely, stone surfaces carried higher proportions of environmental- or soil-associated genera such as *Chromobacterium* ($\Delta = 0.14\%$, $p = 0.0014$), *Micropepsaceae* ($\Delta = 0.32\%$, $p = 0.0032$) and *Haliangium* ($\Delta = 0.68\%$, $p = 0.0068$), while urine showed over-representation of *Acinetobacter* ($\Delta = 4.97\%$, $p < 0.05$) and *Cyanobacteria*. These data indicate that, despite patient-level overlap, stone biofilms selectively accumulate specific environmental taxa absent from contemporaneous urine, underscoring niche-specific microbial partitioning within the same urological ecosystem. The taxa showing significant niche-specific enrichment are illustrated in **Figure 3**.

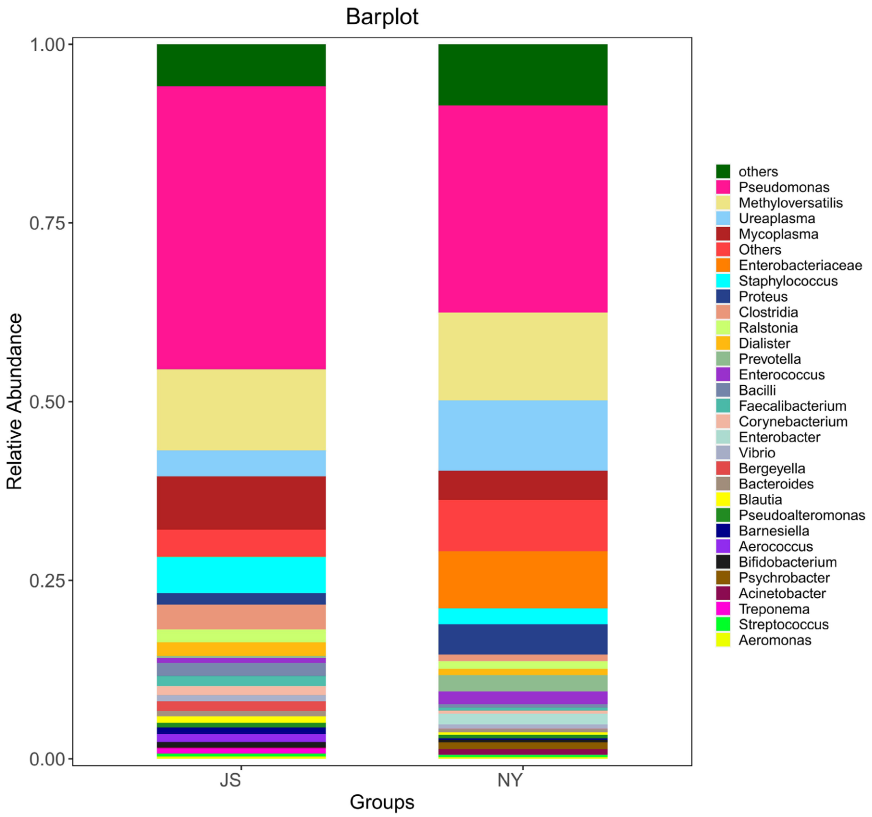
Barplot
Relative Abundance
1.00
0.75
0.50
0.25
0.00
JS
NY
Groups
others
Pseudomonas
Methyloversatilis
Ureaplasma
Mycoplasma
Others
Enterobacteriaceae
Staphylococcus
Proteus
Clostridia
Ralstonia
Dialister
Prevotella
Enterococcus
Bacilli
Faecalibacterium
Corynebacterium
Enterobacter
Vibrio
Bergeyella
Bacteroides
Blautia
Pseudoalteromonas
Barnesiella
Aerococcus
Bifidobacterium
Psychrobacter
Acinetobacter
Treponema
Streptococcus
Aeromonas

(A)

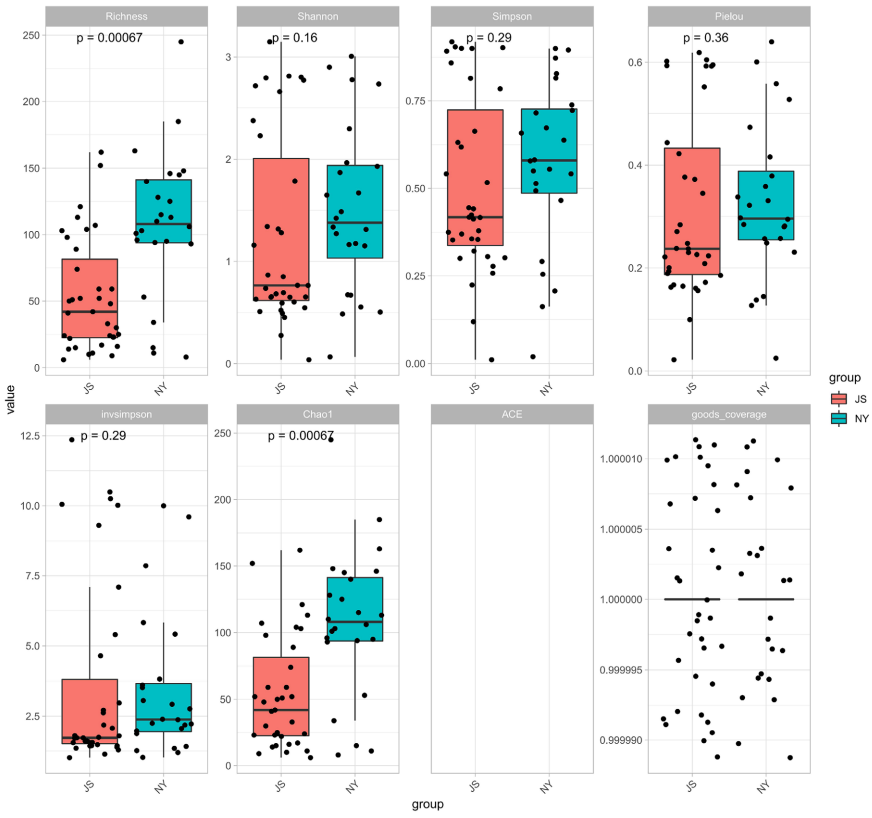
Richness
p = 0.00067
Shannon
p = 0.16
Simpson
p = 0.29
Pielou
p = 0.36
invsimpson
p = 0.29
Chao1
p = 0.00067
ACE
goods_coverage
value
group
JS
NY

(B)

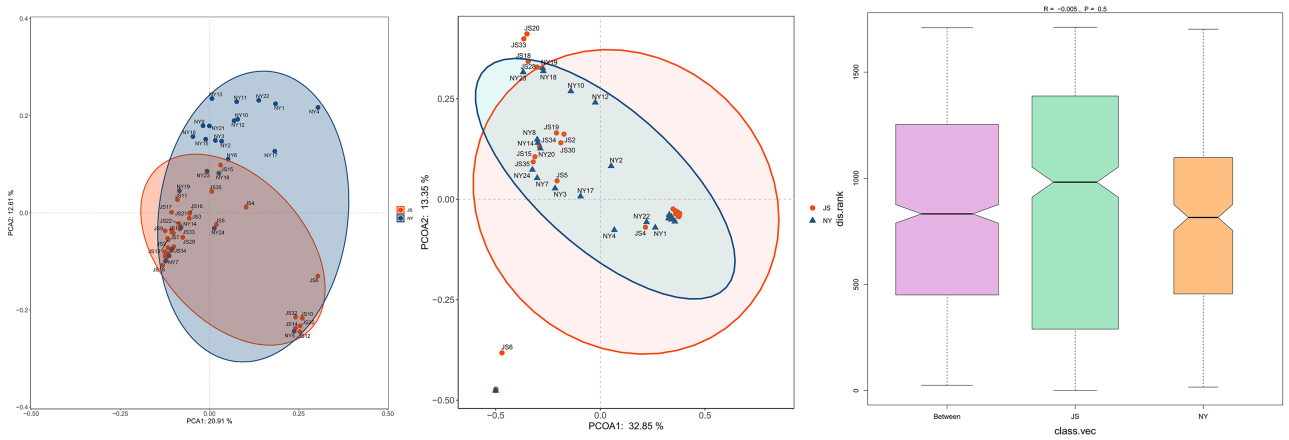

(C)

Figure 2. Diversity analysis of stone (JS) and urine (NY) microbiomes. (A) Boxplots showing the relative abundance of dominant bacterial genera in stone (JS series) and urine (NY series) samples. (B) Boxplots of alpha diversity indices (Shannon and Chao1) for stone and urine samples ($p < 0.05$, Wilcoxon test). (C) Constrained PCoA (Principal Coordinate Analysis) based on Bray-Curtis distances, showing significant separation between stone-surface (JS, blue) and urine (NY, red) microbiomes.

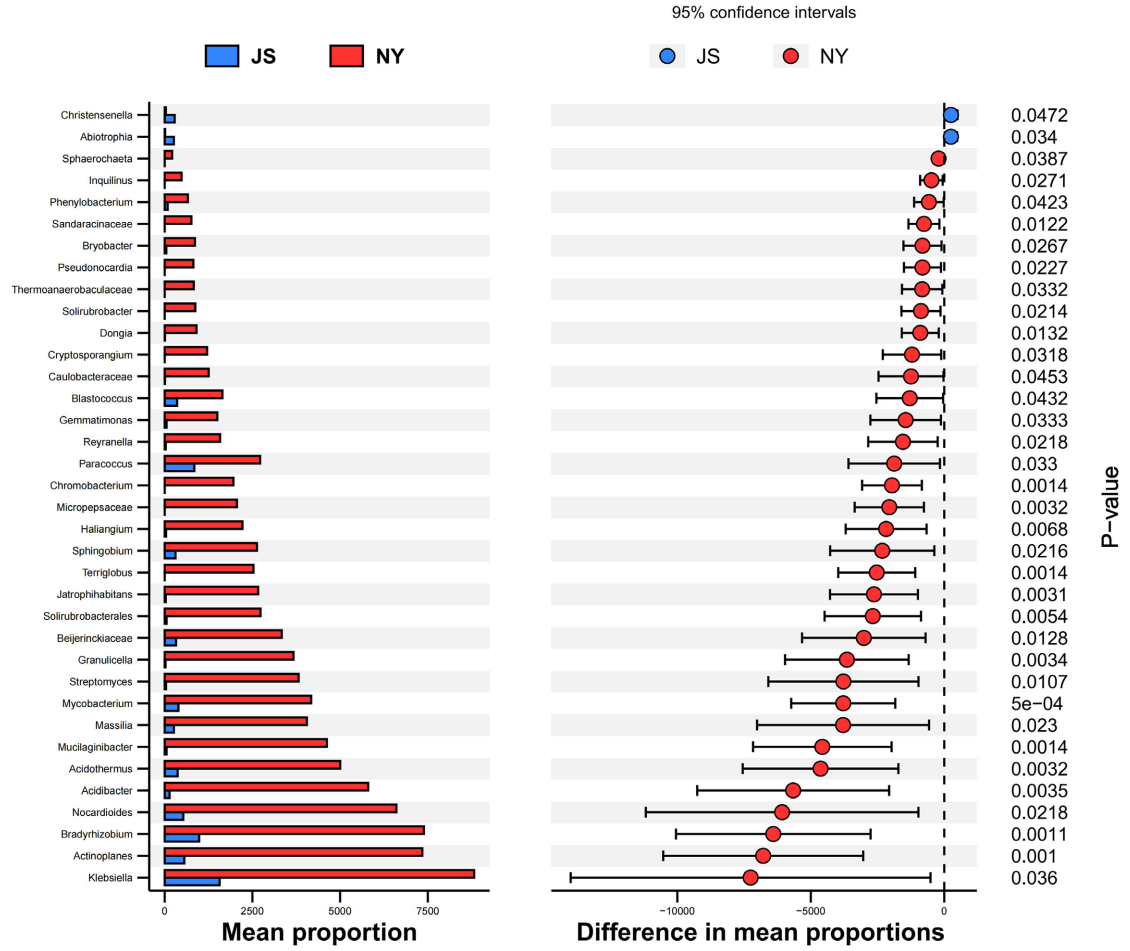

Figure 3. Differential abundance of bacterial taxa between stone (JS) and urine (NY) niches. Bar plot of significantly enriched genera in stones (e.g., Chromobacterium, Haliangium) versus urine (e.g., Acinetobacter, Cyanobacteria). Error bars represent 95% confidence intervals (*p* < 0.05, STAMP analysis).

4. Discussion

This study comprehensively characterized the microbiome of urinary stones and paired urine samples, revealing distinct yet interconnected ecological niches. Stone biofilms demonstrated enrichment of environmental taxa such as Chromobacterium and Haliangium, while urine samples were dominated by conventional uropathogens including Klebsiella and Acinetobacter. Gender-specific patterns emerged, with Mycoplasma/Ureaplasma infections showing marked female predominance and association with inflammatory markers, whereas Group 2 showed lower urinary pH and the highest median crystal value as a descriptive pattern. Microbial distribution patterns further confirmed niche specialization, evidenced by the stone-selective abundance of Christensenella contrasted with urine-enriched Cyanobacteria. Because stone-surface swabs are low-biomass specimens and dedicated blank-control sequencing data were not available in the submitted dataset, low-abundance environmental taxa should be interpreted conservatively.

The distinct microbial partitioning observed between stones and urine corroborates previous findings on biofilm-mediated stone colonization [17]. The preferential enrichment of environmental taxa on stone surfaces suggests these mineralized matrices may provide unique ecological niches for biofilm-adapted bacteria. In contrast, the dominance of motile, planktonic-growing uropathogens like Klebsiella and Acinetobacter in urine aligns with their established roles in urinary tract infections [18]. This clear ecological differentiation highlights the necessity of analyzing both stone-associated and urinary microbiomes to fully elucidate urolithiasis pathogenesis.

The present dataset does not demonstrate a direct mechanistic link between Pseudomonas, urinary alkalinization, and struvite risk. In fact, Group 2 showed the lowest median urinary pH rather than a clear alkalinization pattern, and the crystal-examination comparison did not reach statistically significant pairwise support. Accordingly, any relationship between Pseudomonas, urinary chemistry, and stone formation should be treated as hypothesis-generating rather than causal, and alternative explanations such as stone composition, co-colonizing urease-positive organisms, or host factors remain plausible. Pseudomonas may still reflect an infection-associated urinary niche with biofilm-related persistence, whereas classical struvite pathogenesis is more strongly linked to urease-producing organisms and alkaline urine [19] [20]. Conversely, the pronounced female predominance of Mycoplasma/Ureaplasma infections and their associated inflammatory profiles likely reflects gender-specific anatomical and hormonal susceptibility factors [21]. Of particular note, while pathogen distribution varied significantly between groups, the comparable total bacterial loads across samples suggest that microbial composition may contribute more strongly than total biomass to the observed clinical patterns [22].

The combination of 16S rRNA sequencing with constrained PCoA analysis effectively resolved niche-specific microbiome differences, supporting the growing consensus for comprehensive analytical approaches in stone research [8]. While

distinct microbial clustering was observed, the partial overlap in PCoA space suggests potential bidirectional exchange between stones and urine [23]. These findings highlight the need for future investigations employing shotgun metagenomics to profile functional metabolic pathways, particularly those involved in ureolysis and biofilm formation, complemented by longitudinal sampling to delineate microbial community dynamics throughout stone pathogenesis [24].

Several important limitations should be considered when interpreting our findings. First, the observational nature of this study prevents us from establishing causal relationships between microbial colonization patterns and stone development. Second, while our sample size was robust for common taxa, it may have been inadequate to fully characterize rare microorganisms that could play meaningful roles in lithogenesis. Third, we lacked complete clinical metadata regarding factors like recent antibiotic use and dietary habits, which are known to influence urinary microbiomes. Fourth, dedicated extraction blanks, PCR blanks, and swab-control sequencing data were not available in the current dataset, so low-biomass environmental taxa should be interpreted cautiously [12] [13]. Fifth, although the study design was paired, a full patient-blocked statistical reanalysis could not be reconstructed from the available intermediate analysis files in this revision [25]. Finally, our bacterial-focused 16S rRNA approach did not assess potential viral or fungal contributions to stone formation. These limitations underscore the need for larger longitudinal studies incorporating broader microbial detection methods, stricter low-biomass contamination control, paired-sample statistical modeling, and more comprehensive clinical data collection.

The identification of stone-enriched microbes such as *Christensenella* and *Chromobacterium* opens new possibilities for microbiome-based diagnostic approaches in urolithiasis. These microbial signatures could complement existing clinical tools to improve stone characterization and risk stratification. From a therapeutic perspective, targeting niche-specific microbial vulnerabilities may offer novel strategies for prevention and treatment. By integrating principles of microbial ecology with urological practice, this work lays the foundation for more personalized management strategies in stone disease.

5. Conclusion

This study provides a comprehensive analysis of the distinct microbial ecosystems in urinary stones and paired urine samples, suggesting niche-specific colonization patterns rather than establishing definitive mechanistic relationships. Stone biofilms were predominantly enriched with environmental bacteria such as Christensenella and Chromobacterium, while urine samples were dominated by uropathogens like Klebsiella and Acinetobacter. Notably, gender-specific associations were observed, with Mycoplasma and Ureaplasma infections showing a strong female predominance and Group 2 showing lower urinary pH together with a higher median crystal value in descriptive analysis. The findings underscore the importance of dual microbiome analysis in understanding urolithiasis pathogenesis, as micro-

bial communities in stones and urine exhibit both ecological divergence and potential interactions. Future research should explore functional mechanisms underlying microbial colonization and their direct roles in stone formation, paving the way for personalized interventions in urolithiasis.

Ethical Approval

The study was approved by the Human Research Ethics Committees of the Medical School of Soochow University (Reference 2020CS017). All specimens were collected according to the guidelines set by the Suzhou BenQ Medical Center.

Informed Consent Statement

All authors confirm that all methods were performed in accordance with the relevant guidelines and regulations (Declaration of Helsinki). Written informed consents were obtained from all enrolled patients before specimen collection.

Consent for Publication

Not applicable.

Availability of Data and Materials

The raw data supporting this study will be deposited in a public repository upon acceptance of the manuscript, and the accession number will be provided in the final published version. Processed data supporting the findings of this study are available from the corresponding author upon reasonable request.

Funding

This study was supported by the Project of Suzhou Key Laboratory of Geriatric Intelligent nursing and health preservation.

Authors' Contributions

YG, SY, HL, ZZ, XW wrote the main manuscript text. TL, YG, SY, XW prepared the figures and tables. All authors reviewed the manuscript.

Acknowledgements

Not applicable.

Conflicts of Interest

The authors declare no conflicts of interest.

References

[1] Espinosa-Ortiz, E.J., Eisner, B.H., Lange, D. and Gerlach, R. (2019) Current Insights into the Mechanisms and Management of Infection Stones. *Nature Reviews Urology*, **16**, 35-53. https://doi.org/10.1038/s41585-018-0120-z

[2] Medina, M. and Castillo-Pino, E. (2019) An Introduction to the Epidemiology and

Burden of Urinary Tract Infections. *Therapeutic Advances in Urology*, **11**, Article 1756287219832172. https://doi.org/10.1177/1756287219832172

[3] Kumar, M.S. and Das, A.P. (2016) Molecular Identification of Multi Drug Resistant Bacteria from Urinary Tract Infected Urine Samples. *Microbial Pathogenesis*, **98**, 37-44. https://doi.org/10.1016/j.micpath.2016.06.029

[4] Razi, A., Ghiaei, A., Dolatabadi, F.K. and Haghighi, R. (2024) Unraveling the Association of Bacteria and Urinary Stones in Patients with Urolithiasis: An Update Review Article. *Frontiers in Medicine*, **11**, Article 1401808. https://doi.org/10.3389/fmed.2024.1401808

[5] Amano, M. and Shimizu, T. (2014) Emphysematous Cystitis: A Review of the Literature. *Internal Medicine*, **53**, 79-82. https://doi.org/10.2169/internalmedicine.53.1121

[6] Wang, Z., Zhang, Y., Zhang, J., Deng, Q. and Liang, H. (2021) Recent Advances on the Mechanisms of Kidney Stone Formation (Review). *International Journal of Molecular Medicine*, **48**, Article No. 149. https://doi.org/10.3892/ijmm.2021.4982

[7] Papatsoris, A., Alba, A.B., Galán Llopis, J.A., Musafer, M.A., Alameedee, M., Ather, H., *et al*. (2024) Management of Urinary Stones: State of the Art and Future Perspectives by Experts in Stone Disease. *Archivio Italiano di Urologia e Andrologia*, **96**, Article 12703. https://doi.org/10.4081/aiua.2024.12703

[8] Kachroo, N., Lange, D., Penniston, K.L., Stern, J., Tasian, G., Bajic, P., *et al*. (2021) Standardization of Microbiome Studies for Urolithiasis: An International Consensus Agreement. *Nature Reviews Urology*, **18**, 303-311. https://doi.org/10.1038/s41585-021-00450-8

[9] Lemberger, U., Pjevac, P., Hausmann, B., Berry, D., Moser, D., Jahrreis, V., *et al*. (2023) The Microbiome of Kidney Stones and Urine of Patients with Nephrolithiasis. *Urolithiasis*, **51**, Article No. 27. https://doi.org/10.1007/s00240-022-01403-5

[10] Hong, S.Y., Yang, Y.Y., Xu, J.Z., Xia, Q.D., *et al*. (2022) The Renal Pelvis Urobiome in the Unilateral Kidney Stone Patients Revealed by 2bRAD-M. *Journal of Translational Medicine*, **20**, Article No. 431. https://doi.org/10.1186/s12967-022-03639-6

[11] Hobbs, T., Schultz, L.N., Lauchnor, E.G., Gerlach, R. and Lange, D. (2018) Evaluation of Biofilm Induced Urinary Infection Stone Formation in a Novel Laboratory Model System. *Journal of Urology*, **199**, 178-185. https://doi.org/10.1016/j.juro.2017.08.083

[12] Salter, S.J., Cox, M.J., Turek, E.M., Calus, S.T., Cookson, W.O., Moffatt, M.F., *et al*. (2014) Reagent and Laboratory Contamination Can Critically Impact Sequence-Based Microbiome Analyses. *BMC Biology*, **12**, Article No. 87. https://doi.org/10.1186/s12915-014-0087-z

[13] Eisenhofer, R., Minich, J.J., Marotz, C., Cooper, A., Knight, R. and Weyrich, L.S. (2019) Contamination in Low Microbial Biomass Microbiome Studies: Issues and Recommendations. *Trends in Microbiology*, **27**, 105-117. https://doi.org/10.1016/j.tim.2018.11.003

[14] Bailén, M., Bressa, C., Larrosa, M. and González-Soltero, R. (2020) Bioinformatic Strategies to Address Limitations of 16rRNA Short-Read Amplicons from Different Sequencing Platforms. *Journal of Microbiological Methods*, **169**, Article 105811. https://doi.org/10.1016/j.mimet.2019.105811

[15] Estaki, M., Jiang, L., Bokulich, N.A., McDonald, D., González, A., Kosciolek, T., *et al*. (2020) QIIME 2 Enables Comprehensive End-to-End Analysis of Diverse Microbiome Data and Comparative Studies with Publicly Available Data. *Current Protocols in Bioinformatics*, **70**, e100. https://doi.org/10.1002/cpbi.100

[16] Parks, D.H., Tyson, G.W., Hugenholtz, P. and Beiko, R.G. (2014) STAMP: Statistical

Analysis of Taxonomic and Functional Profiles. *Bioinformatics*, **30**, 3123-3124. https://doi.org/10.1093/bioinformatics/btu494

[17] Tenke, P., Köves, B., Nagy, K., Hultgren, S.J., Mendling, W., Wullt, B., *et al.* (2012) Update on Biofilm Infections in the Urinary Tract. *World Journal of Urology*, **30**, 51-57. https://doi.org/10.1007/s00345-011-0689-9

[18] Tarnagda, H., Ouermi, D., Sagna, T., Nadembega, W.M.C., Ouattara, A.K., Traoré, L., *et al.* (2024) Prevalence and Antibiotic Resistance of Urinary Tract Pathogens, with Molecular Identification of *Klebsiella pneumoniae*, *Klebsiella oxytoca*, and Acinetobacter spp., Using Multiplex Real-Time PCR. *American Journal of Molecular Biology*, **14**, 245-260. https://doi.org/10.4236/ajmb.2024.144018

[19] Newman, J.W., Floyd, R.V. and Fothergill, J.L. (2017) The Contribution of Pseudomonas Aeruginosa Virulence Factors and Host Factors in the Establishment of Urinary Tract Infections. *FEMS Microbiology Letters*, **364**.

[20] Flannigan, R., Choy, W.H., Chew, B. and Lange, D. (2014) Renal Struvite Stones—Pathogenesis, Microbiology, and Management Strategies. *Nature Reviews Urology*, **11**, 333-341. https://doi.org/10.1038/nrurol.2014.99

[21] Combaz-Söhnchen, N. and Kuhn, A. (2017) A Systematic Review of Mycoplasma and Ureaplasma in Urogynaecology. *Geburtshilfe und Frauenheilkunde*, **77**, 1299-1303. https://doi.org/10.1055/s-0043-119687

[22] Zaura, E., Keijser, B.J., Huse, S.M. and Crielaard, W. (2009) Defining the Healthy "Core Microbiome" of Oral Microbial Communities. *BMC Microbiology*, **9**, Article No. 259. https://doi.org/10.1186/1471-2180-9-259

[23] Ticinesi, A., Milani, C., Guerra, A., Allegri, F., Lauretani, F., Nouvenne, A., *et al.* (2018) Understanding the Gut-Kidney Axis in Nephrolithiasis: An Analysis of the Gut Microbiota Composition and Functionality of Stone Formers. *Gut*, **67**, 2097-2106. https://doi.org/10.1136/gutjnl-2017-315734

[24] Seneviratne, C.J., Suriyanarayanan, T., Widyarman, A.S., Lee, L.S., Lau, M., Ching, J., *et al.* (2020) Multi-Omics Tools for Studying Microbial Biofilms: Current Perspectives and Future Directions. *Critical Reviews in Microbiology*, **46**, 759-778. https://doi.org/10.1080/1040841x.2020.1828817

[25] Khomich, M., Måge, I., Rud, I. and Berget, I. (2021) Analysing Microbiome Intervention Design Studies: Comparison of Alternative Multivariate Statistical Methods. *PLOS ONE*, **16**, e0259973. https://doi.org/10.1371/journal.pone.0259973